

Real-time ocean chemistry for improved biogeochemical observation in dynamic coastal environments

Alan M. Volpe*, Bradley K. Esser

Lawrence Livermore National Laboratory, P.O. Box 808, L-016, Livermore, CA 94550, USA

Accepted 11 March 2002

Abstract

We describe a new ocean observation system that integrates mass spectroscopy, hydrographic instrumentation, and satellite imagery (SeaWiFS). We used a quadrupole ICP mass spectrometer at sea to acquire continuous trace element data during separate surveys of the Baja California coastal margin, and the San Diego Bay and coastal environment. There is evidence for extreme Ba depletion in surface waters off the Baja coast, which is the result of biological productivity and marine barite precipitation. The synoptic data are used to elucidate the biochemical mechanism of barium removal; to constrain the spatial and temporal boundaries over which the phenomenon occurs; and to quantify surface flux to sediments. Further systems application led to mapping of the distribution of a suite of biologically active trace metals (Mn, Ni, Zn, Cu, and Cd) in San Diego Bay, and the Bay signature was tracked in tidal plumes into the coastal ocean. The continuous data provided chemical gradients within the Bay, with which we estimate the contaminant metal flux that is discharged from the Bay into the coastal ocean during tidal pumping. © 2002 Elsevier Science B.V. All rights reserved.

Keywords: Ocean science; Mass spectrometry; Trace elements; Micronutrients; Productivity; Regional index, Northeast Pacific; Baja California; San Diego Bay

1. Introduction

Oceans and coastal ecosystems are vital to the health and sustenance of people all over the world. Mankind is exerting tremendous pressure on coastal oceans through over-fishing, land runoff, waste disposal, spills, and destruction of habitats. Interdisciplinary research has led to an understanding of the interplay among physical, biological, geological, and chemical processes that control the complex

exchanges in ocean waters (Butler, 1998; Falkowski et al., 1998; Jickells, 1998; McGowan et al., 1998; Uppenbrink et al., 1998; Mason, 2001). Until recently, marine geochemical measurements involved analysis of a single analyte made on discrete bottle samples. Although important for allowing a first-order characterization, such an analytical and sampling strategy yields a record that is discontinuous in time and space. In dynamic coastal environments, this record is inadequate for quantifying the fluxes and impact of anthropogenic inputs on the coastal biosphere.

To address the issue of undersampling for trace metals in the coastal ocean, we took a system

* Corresponding author. Tel./fax: +1-925-423-4261.
E-mail address: volpe1@llnl.gov (A.M. Volpe).

approach to measure chemical composition at high spatial resolution, and developed an integrated system of in-situ real time analytical instruments. This system included a trace element capability based on inductively coupled plasma mass spectrometry (ICPMS) instrumentation (Volpe et al., 2001) and nonhazardous methods for rapidly concentrating gamma-ray emitting radioisotopes (Bandong et al., 2001) that was integrated with traditional oceanographic sensors and fluorometers on a towed body. ICPMS is a proven technology for inorganic analysis, and it is an appropriate technology to adapt for at-sea operation, because it achieves low detection levels at the parts-per-trillion (one in 10^{12}) level with high precision and accuracy (1% or better). The technologic challenge we met was to deliver high sensitivity measurements of trace elements at a rate rapid enough to acquire large spatially and temporally continuous data sets (Volpe et al., 2001). This integrated capability is an advancement in our ability to observe phenomena affecting marine biology and chemistry that directly addresses the technological challenges set forth by the National Academy of Sciences (NRC, 1998) for improvement in ocean observation. It can be incorporated with other regional ocean studies (Boyd and Law, 2001; Dickey et al., 2001; Koeve and Ducklow, 2001), which would benefit from additional at-sea analytical measurements.

The purpose of this paper is to describe the integrated analytical system, and then show how the trace element and isotope data can be used in a system approach to better understand biogeochemical coastal processes. We discuss real-time ocean chemical measurements acquired during two at-sea experiments with synoptic hydrographic data and chlorophyll *a* concentration derived from satellite ocean color radiance (SeaWiFS). The first experiment was conducted off the coast of Baja California. It provided insight to the coupling between rapid changes in biological productivity and removal of Ba, which serves as a proxy for biological productivity, from surface water (Esser and Volpe, in press (a)). The lack of significant input from rivers, rain, or groundwater makes the Pacific Ocean off Baja California an ideal location for studying the effects of coastal productivity on barium cycling.

The second experiment involved in-situ trace transition metal (Mn, Ni, Cu, Zn, and Cd) characterization of San Diego Bay water, and real-time tracking of this

effluent plume offshore through the San Diego Bight during tidal flushing. San Diego Bay ranks as one of the most contaminated coastal areas in the nation. This ranking is based on high levels of organic and metal pollutants in sediments and fish, and demonstrated biological effects in fish (Martin, 1985; McCain et al., 1992). San Diego Bay is also a significant source of pollutant metals to the adjoining coastal ocean. Quantifying the flux of metals out of the Bay is important in determining the major sources and sinks of pollutant metals in the heavily impacted Southern California Bight.

2. Methods and data

2.1. Field programs

We performed extended at-sea tests of the ICPMS equipment from October 17 to November 4, 1998 aboard the *R/V Roger Revelle* on an expedition to the Alarcon Basin in the Gulf of California (Fig. 1). Though the primary objective was to study geophysical and geochemical aspects of the ocean spreading ridge in the Gulf of California, the expedition provided an extremely cost-effective opportunity to conduct at-sea evaluation of instrumentation. Measurement and testing of the ICPMS and ancillary equipment was performed in a specially outfitted analytical van on the aft-deck of the *R/V Revelle*. To our knowledge, this experiment was the first at-sea deployment and use of a quadrupole ICP mass spectrometer.

The ICPMS operated daily (12 days) and met all performance criteria for land-based mass spectrometry operation (Volpe et al., 2001) while the ship transited to the Gulf of California and during geophysical surveys that were conducted in the Alarcon Basin. On the northern transit from the Alarcon Basin to San Diego (Fig. 1), the ICPMS operated continuously for 66 h, and returned over 3500 discrete Ba and Mo measurements. At an average ship speed of 12 knots, the spatial resolution of the trace metal and hydrographic data across nearly 1500 km of coastal water was about 370 and 10 m, respectively. Though trace element and hydrographic data were available real time during this northward transit, prior science scheduling and deployment of a towed seismic array

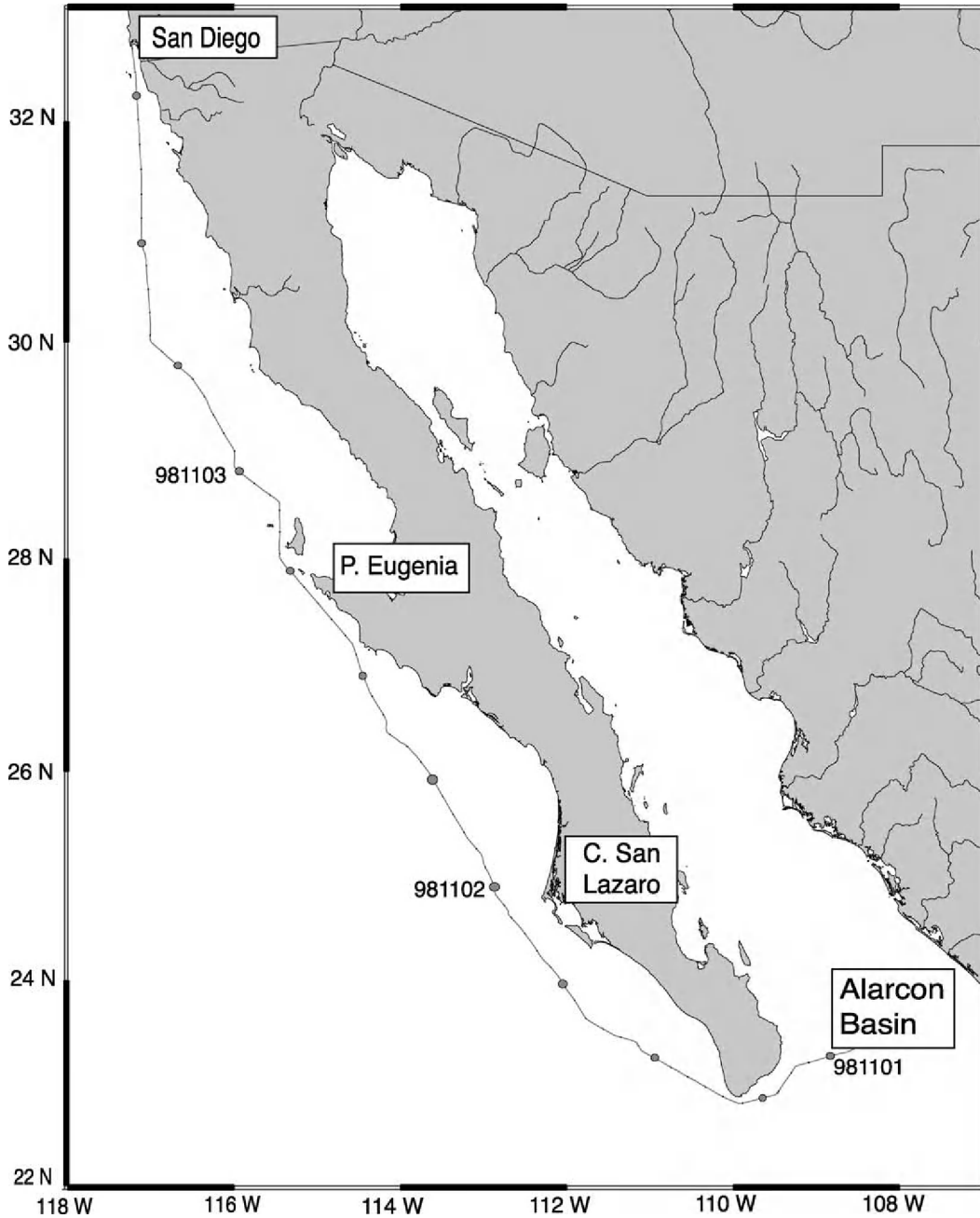


Fig. 1. *R/V Revelle* ship track on the 3-day northward transit from the Alarcon Basin to San Diego. Calendar dates (yyymmdd) are shown at the start of the day (00:00 GMT) with circles indicating ship position at 6-h intervals.

precluded deployment of another towed body, or deviation from course (i.e., other experiments drove the ship). The hydrographic sensor system was sus-

pending vertically in a light-tight stainless steel tank. Ocean water was pumped through the tank from the ship's clean water intake, which is located in the bow

of the *Revelle*, approximately 5 m below water line. Additional water from this intake was plumbed to the iso-van for trace element analysis. Contamination studies conducted during hydrocasts in the Alarcon basin confirmed little effect from ship intake on a suite of trace elements including Ba and Mo.

At-sea science experiments in the San Diego Bay and coastal margin were conducted September 13–17, 1999 aboard the *R/V Robert G. Sproul* using the same ICPMS and support analytical van. The purpose of these experiments was the scientific application of an enhanced analytical system as a first step towards full chemical characterization of the

impact of harbor, bay, and lagoon outflow on coastal waters around San Diego (Fig. 2). In this experiment, the hydrographic sensor system was deployed on a towed body. A titanium and Teflon gear pump on the towed body delivered seawater through Teflon tubing, which was part of the electromechanical cable, to the shipboard analytical lab for myriad chemical analyses.

The ICPMS was used to quantify elemental composition of waters in Southern California embayments and the coastal zone in conjunction with simultaneous sampling of invertebrate larvae (crabs, barnacles, bivalves), chlorophyll, and dissolved organic carbon

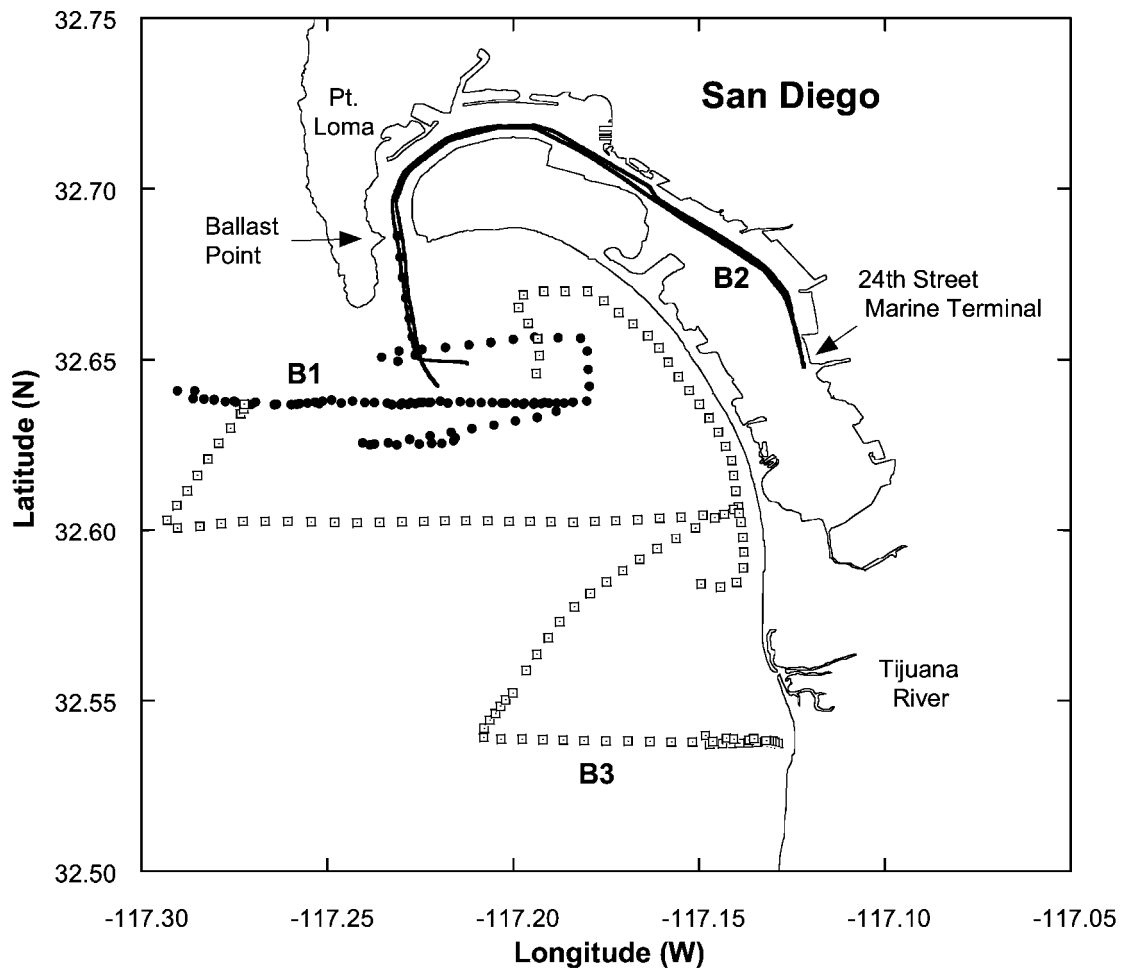


Fig. 2. *R/V Sproul* ship tracks showing surveys conducted in and around San Diego Bay (B1–B3) during 15–16 September 1999. B1 (closed circles) survey was around Bay entrance at 32.64°N; B2 (solid line) survey was inside San Diego Bay to the southern end of the Bay, and back; B3 (open squares) survey included the Coronado coast and two east–west transits at 32.60°N and 32.55°N.

(Gieskes et al., in preparation). We mapped Mn, Ni, Cu, Zn, and Cd in San Diego Bay from the entrance to the southern portion of the bay (Fig. 2; B2), and in the coastal ocean of the San Diego Bight (Fig. 2; B1, and B3).

2.2. Satellite imagery

Satellite images showing surface chlorophyll *a* concentration measured by the sea-viewing wide field-of-view sensor (SeaWiFS) were obtained from the NASA Goddard Distributed Active Archive Center. Images were examined from October 16 to November 8, 1998 for the regional survey off Baja California, and September 7–14, 1999 for the survey of San Diego Bay and adjacent coastal waters. SeaWiFS Level 1A LAC data files for October 31 and November 2, 1998, acquired by the Monterey Bay Aquarium Research Institute HRPT station HMBR, were obtained from the Goddard Earth Sciences Distributed Active Archive Center (GES DAAC) archive. The files were processed to Level 2 to generate chlorophyll *a* concentrations using SeaDAS Version 4.0. Default atmospheric correction parameters were used. The standard chlorophyll *a* concentration palette was modified to emphasize the chlorophyll *a* variability over the concentration range found in this region. The ship track and coastline were overlain on the image using SeaDAS functions. Maximum pixel resolution for SeaWiFS LAC data is 1 km at nadir.

The remote sensing of ocean color from space allows estimation of chlorophyll *a* concentration, which can provide information on the abundance of phytoplankton in surface ocean waters. Ocean color data can also be used to detect the presence of dissolved and particulate species in surface water. Ocean color data are therefore valuable in interdisciplinary research involving terrigenous runoff, physical transport, and biological productivity in coastal ocean ecosystems. However, the images are dependent on the algorithms used to derive pigment concentration and other geophysical variables from measured radiance. The SeaWiFS algorithm generally overestimates the chlorophyll *a* concentration in turbid and organic-rich waters flushed from coastal bays and harbors like San Diego Bay (i.e., Case II water).

2.3. Hydrographic and nutrient data

Oceanographic data were collected using a Seabird Electronics (Bellvue, WA) SBE 911+ underwater CTD system on a towed body that was outfitted with a Chelsea Aquatracka UV-fluorometer, a WETLabs chlorophyll fluorometer, a Sea Tech transmissometer, and a Seapoint turbidity meter. Temperature ($^{\circ}\text{C}$), salinity, FDOM ($\mu\text{g/l}$), chlorophyll ($\mu\text{g/l}$), and light transmittance (%) data were acquired every 1.5 s during the surveys. The data were filtered using a moving median ($n=11$) algorithm to remove spikes, and the plotted data were averaged over 30 s using a moving ($n=20$) average algorithm.

The UV-fluorometer that measured FDOM used a pulsed 239-nm excitation light source, and a photomultiplier for the detection of fluorescent organic matter at 440-nm wavelength emission. The transmissometer measured light transmission across a 25-cm water path length using a modulated LED and a synchronous detector. The WETLabs chlorophyll fluorometer used a blue light (455 nm) excitation source, and measured red light (685 nm) emission. The electronic responses of the UV-fluorometer and chlorophyll fluorometer were calibrated with solutions of quinine sulfate and coproporphyrin, respectively.

Chlorophyll absorbs blue light and re-emits a portion of this light as fluorescence at a longer wavelength. Characterization of the voltage output was performed using a standard solution containing 0.5 mg of coproporphyrin methyl ester dissolved in 20 ml of 6 M HCl and 980 ml of deionized water. A suite of standard dilutions was used to determine linearity of the response. This 0.5 mg/l coproporphyrin solution is nominally equivalent to 50 $\mu\text{g/l}$ of chlorophyll, though absolute values are estimates at best, since the fluorometer was not calibrated using known chlorophyll species or standards. However, during the San Diego Bay experiment, there was good correlation between the values obtained from the fluorometer and the sum of chlorophyll and pheophytin (E. Renger, SIO) measured using laboratory methods (Gieskes et al., in preparation). The ratio of fluorometer to lab measurement was 2.2 for San Diego Bay surface waters having chlorophyll plus pheophytin concentrations between 2 and 8.5 mg/m^3 .

Salinity values were calibrated with bottle samples collected during the experiments and analyzed at the

Oceanographic Data Facility (SIO). The ratios of lab to field (salinometer/CTD) salinity measurements have an average value of 1.000 with an uncertainty of 0.1%. Filtered (0.45 μm) water samples for laboratory analysis of silica, nitrate, and phosphate (nutrients) were collected hourly in a HEPA-filtered glove box, and analyzed at the Oceanographic Data Facility (SIO).

2.4. Trace elements—ICPMS

Components of the ICPMS capability were evaluated during extended at-sea experiments aboard the *R/V Revelle* on the Alarcon expedition (Volpe et al., 2001), and in San Diego Bay aboard the *R/V Robert Gordon Sproul* (Esser and Volpe, in press (b)). During the experiments the ICPMS operated in a temperature- and environmentally controlled analytical van on the aft deck of each vessel. Instrument operation was similar, but sample processing differed in the experiments. During the survey off the Baja California coast, seawater was processed through an on-line dilution system prior to ICPMS analysis. The survey of trace metals in and around San Diego Bay required on-line separation and extraction methods before analysis. In both field experiments, seawater was filtered (0.45 μm) prior to ICPMS analysis.

2.4.1. On-line dilution

In order to analyze trace elements, such as Ba and Mo in seawater at the nanomolar level, at rapid analytical rates, an on-line dilution and internal standardization system was fabricated (Volpe et al., 2001). Simple dilution of seawater, rather than matrix elimination ion exchange and analyte preconcentration, is possible because Ba and Mo concentrations are high (10–100 nmol/l) relative to ICPMS sensitivity (<0.01 nmol/l). Also, there is little molecular interference from major and minor ions present in seawater on the isotopes of Ba and Mo. The on-line system mixed filtered (0.45 μm) seawater with a diluent containing internal standard elements, and then delivered the mixed solution directly to the ICPMS plasma source interface. The optimal dilution factor was determined by the trade-off between loss of signal due to dilution effects and the loss of signal due to matrix effects. Measured mixing ratios were consistently 22 parts diluent to 1 part seawater. Dilution and

mixing of discrete samples, such as the calibration standards, were identical to the on-line seawater method. Molybdenum is normalized to the same internal standard as Ba, and it was measured to monitor internal standard corrections and dilution ratio stability (Volpe et al., 2001). For this experiment, Mo is considered a conservative element in seawater, since the ratio of Mo to salinity is uniform within the combined analytical uncertainty (1–2%) of the ICPMS and the conductivity meter.

Each ICPMS data acquisition took about 36 s per repetition, including settle times between masses. Data reduction and processing sequence information took an additional 20 s, for a total analytical cycle of 1 min. For each element, concentration was determined by external calibration against the appropriate set of calibration standards using a simple linear calibration curve after internal standardization against the nearest internal standard mass. Six-hour performance tests in surface water of the Gulf of California with uniform salinity (35.00 ± 0.03) prior to the return transit indicated that internally standardized signals averaged over 5 min were highly reproducible; Mo ($2\sigma = 1.8\%$), and Ba ($2\sigma = 4\%$).

2.4.2. On-line pre-concentration

First series transition metals are typically present at picomolar to nanomolar levels in open ocean surface water, though their abundance can increase significantly in coastal areas due to pollution and flux from rivers and sediments. In addition, major and minor ions present in seawater cause molecular interference with isotopes of the first series transition metals that have atomic mass between 40 and 80 amu. These factors restrict direct quadrupole ICPMS analysis, and matrix elimination and pre-concentration methods are required for sensitive and accurate measurement of transition series metals in seawater.

Flow injection systems utilizing low-pressure ion chromatography with 8-hydroxyquinoline or iminodiacetic acid resins have been coupled to ICPMS in research laboratories. These techniques are capable of parts per trillion detection limits with turnaround times of a few minutes (Ebdon et al., 1993; Bloxham et al., 1994; DeCarlo and Resing, 1998; Willie et al., 1998). We modified these methods and used Toyopearl® AF-Chelate 650M resin, which is an iminodiacetic acid resin with a macroporous metha-

cryalate backbone, as the ion-exchanger. This resin is commercially available and has been employed to process seawater for pre-concentration and matrix elimination in flow injection ICPMS analysis (Willie et al., 1998). We constructed a column of 1/8-in. OD, 1/16-in. ID Tefzel® tubing and 1/8-in. natural PEEK fittings. The resultant 3-cm column contained approximately 50 µl of resin, and sustained flow rates in excess of 2 ml/min at peristaltic pump pressures. They were easily incorporated into and removed from the flow injection system with standard 1/8-in. chromatography fittings. In addition to the analytic column, clean-up columns, constructed in the same manner, were placed on the buffer line and carrier line to reduce reagent blanks (Esser and Volpe, in press (b)).

An automated flow injection scheme was designed and tested using reference seawater standards from the National Research Council of Canada (Esser and Volpe, in press (b)). Each analysis takes 4 min and processes 3 ml of seawater. The protocol efficiently separates transition metals from seawater matrix ions. Measured seawater isotopic ratios for metals of interest are identical to the same ratios measured in aqueous standards. This indicates the effectiveness of the method to separate transition metals from the saline matrix. In addition to rapid analysis, the technique is sufficiently accurate, precise, and sensitive for high-resolution coastal seawater surveying.

Systematic offsets for Cu were observed between at-sea and laboratory analyses (Esser and Volpe, in press (b)). The Cu concentrations determined at sea in continuously sampled, unacidified seawater are half the concentrations determined in acidified preserved seawater (0.50 ± 0.03), even though both are buffered to the same pH before loading on the column. These observations suggest that only half of the Cu in unacidified seawater is retained by the iminodiacetate resin column. These effects have been attributed to the presence of naturally occurring organic ligands, which in unacidified seawater strongly complex copper and effectively compete with the iminodiacetate functional group (Abdullah et al., 1976; Bruland et al., 1979; Rasmussen, 1981; Paulson, 1986). The existence of organic ligands, which strongly complex a large fraction of total copper in seawater, is well established (Coale and Bruland, 1988, 1990; Donat et al., 1994; Miller and Bruland, 1994; Moffett, 1995; Moffett et al., 1997; Zamzow et al., 1998; Zirino et al., 1998).

Since our data are consistent with such an interpretation, and since differences between Cu measurements at-sea relative to laboratory analysis are consistent (ratio = 0.50 ± 0.03), we have corrected the at-sea data. The plotted Cu data are total dissolved Cu, and may be compared with literature Cu data.

2.5. Gamma-ray emitting isotopes—radiocesium

For several decades, radiocesium has been used as a conservative tracer of water circulation (Kupferman et al., 1979; Livingston, 1988). Large volumes of seawater (>1000 l) were processed through a particle and dissolved ion extraction system during the Alarcon expedition off Baja California aboard the *R/V Revelle* to measure radiocesium, ^{137}Cs . This system isolates coarse suspended particulate material (SPM) greater than 1 µm, fine SPM between 0.1 and 1.0 µm, and a suite of dissolved ions, which are extracted using solid phase sorbent material, such as hexacyanoferrate (Bandong et al., 2001). Total suspended material in surface water off Baja was very low (<1 mg/l). Data collection and analysis focussed only on ^{137}Cs in the dissolved fraction, since it is a conservative, soluble element in offshore waters. Samples were processed during transit to and from San Diego and the Gulf of California (Volpe et al., 2002). All samples were returned to the counting facility at LLNL for gamma spectroscopy analysis.

3. Baja California: coastal productivity and surface chemical flux

3.1. Hydrography

The California Current System extends from Vancouver Island to the tip of Baja California, and is divided into three geographic regions with the Baja Peninsula being the southernmost (Hickey, 1998). The California Current is a major eastern boundary current, which flows equatorward year-round bringing cold Pacific Subarctic water from the north. There have been few current measurements off Baja Peninsula, so variability and forcing mechanisms are not well understood. However, the large-scale wind stress field channeled by mountains that extend the length of the Baja Peninsula leads to

surface water offshore transport, which is replaced by upwelling of deeper water (Bakun and Nelson, 1977; Bakun, 1990).

Continuous hydrographic, nutrient, and barium data (Fig. 3) were collected during the 3-day northern transit from warm waters at the mouth of the Gulf of

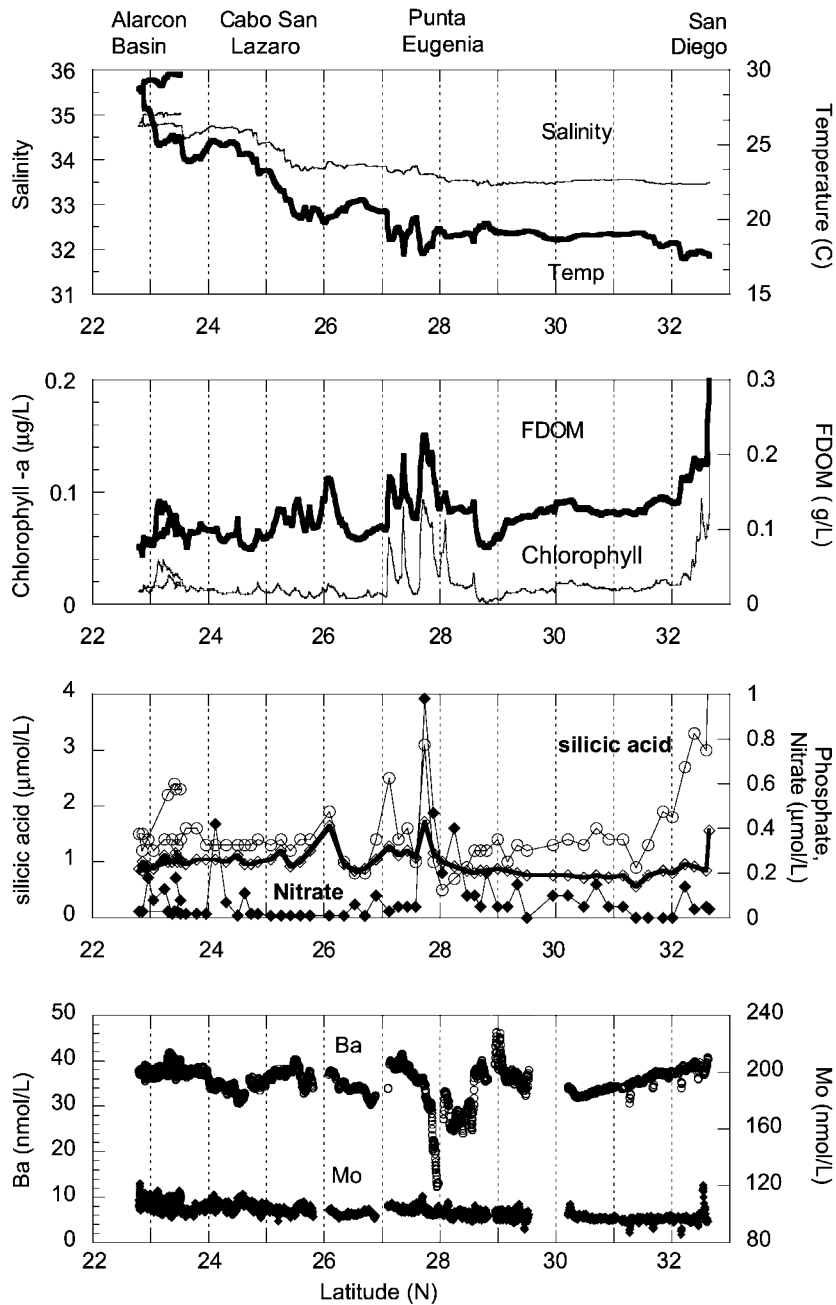


Fig. 3. Plots of oceanographic data (salinity, temperature, FDOM, chlorophyll, nutrients and trace elements) taken aboard the *R/V Revelle* during northward transit along the Pacific Coast of Baja California from the Alarcon Basin to San Diego.

California (23°N), across the Baja California coastal margin to San Diego (32.5°N). About 6 h was spent transiting from the Alarcon Basin to Cabo San Lucas, followed by a 70-h southeast-to-northwest transit to San Diego (Fig. 1). Fig. 3 shows hydrographic, nutrient, and trace element data for the complete transit. Panel 1 shows continuous salinity and temperature ($^{\circ}\text{C}$) data. Panel 2 shows continuous fluorescent dissolved organic matter (FDOM), and chlorophyll data. Hydrographic data were averaged over 30-s time intervals using a running average algorithm. Panel 3 shows silica, nitrate, and phosphate data from bottle samples that were taken hourly and returned for post-cruise analysis. Finally, panel 4 shows continuous

ICPMS data for Ba and Mo, which were collected once per minute and averaged over 5-min intervals.

Major transitions in surface water temperature, salinity, and chemical properties occurred at Cabo San Lucas (22.8°N), Cabo San Lazaro (24.8°N), Punta Eugenia (27.8°N), and in the San Diego Bight near the US–Mexico border (32.5°N). In the Alarcon Basin at the mouth of the Gulf of California, surface water was warm and saline, which is typical of evaporated Equatorial Pacific water (Bray, 1988). Surface circulation in the Baja coastal region between Cabo San Lucas and San Diego was dominated by the California Current and California Countercurrent. These waters form by mixing of Pacific Subarctic,

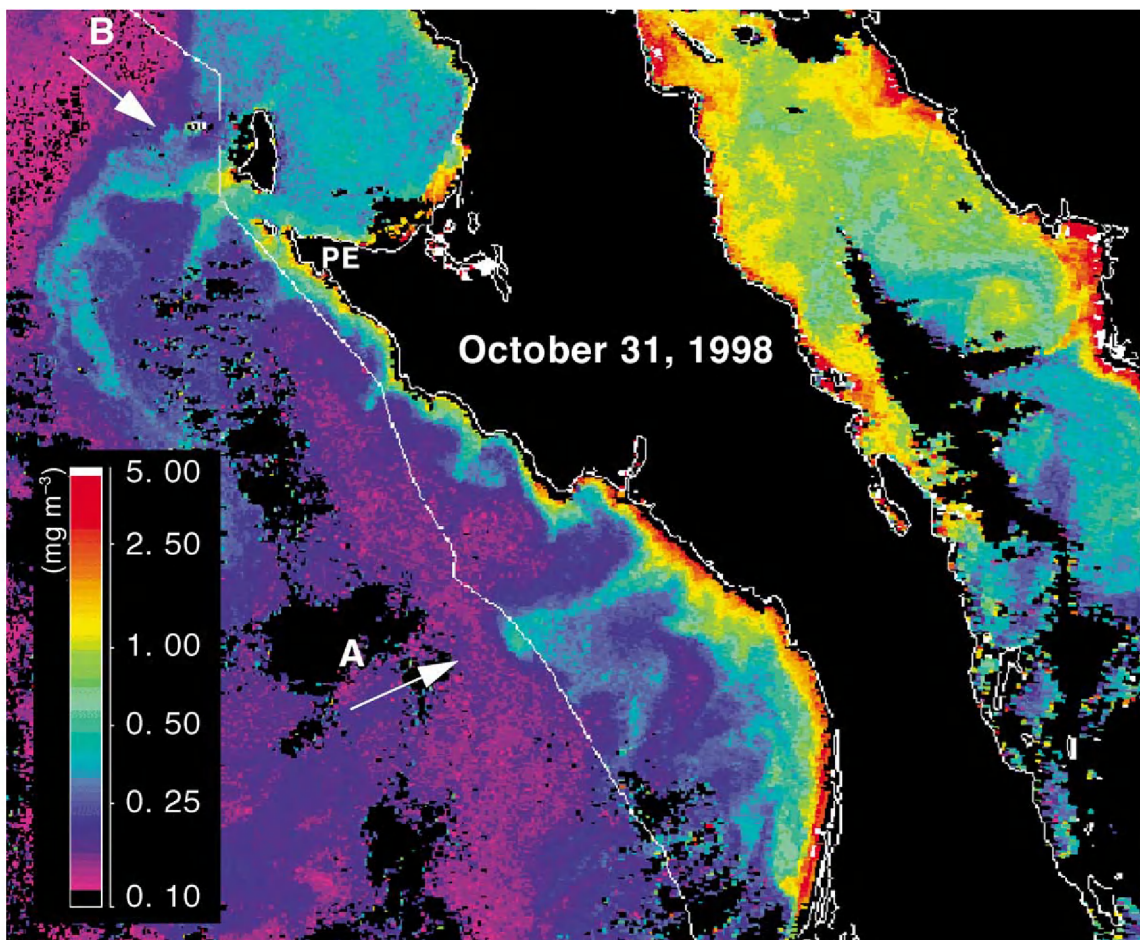


Fig. 4. SeaWiFS ocean color image of chlorophyll for October 31, 1998. Ship track (white line) shows position of the *R/V Revelle* on the northward transit to San Diego from the Gulf of California, on November 2, 1998. Arrows A and B indicate prominent eddies of high chlorophyll *a* content. Image shows relative chlorophyll *a* concentration from low values, 0.10 mg/m^3 (magenta), to high, 5 mg/m^3 (red).

North Pacific Central, Equatorial Pacific, and upwelled coastal water (Lynn and Simpson, 1987; Hickey, 1998). South of Cabo San Lazaro (25°N), the ship crossed into the California Current, and surface water temperature and salinity dropped (Fig. 3). Finally, as the track approached the US–Mexico border (31.8°N), nutrients, chlorophyll, and FDOM increased while temperature dropped 1–2° C (Fig. 3). These variations are related to a sharp onshore component of the California Current system dividing northern eutrophic waters from southern oligotrophic waters (Segovia-Zavala et al., 1998). To the north,

near San Diego Bay (32.5°N), there are pronounced increases in turbidity, FDOM, and chlorophyll that are discussed below.

3.2. Satellite observation

SeaWiFS ocean color images corresponding to chlorophyll *a* concentration in surface water off the coast of Baja California for October 31, 1998 and November 2, 1998 are shown in Figs. 4 and 5, respectively. Chlorophyll *a* concentration derived from satellite imagery, as well as at-sea surface

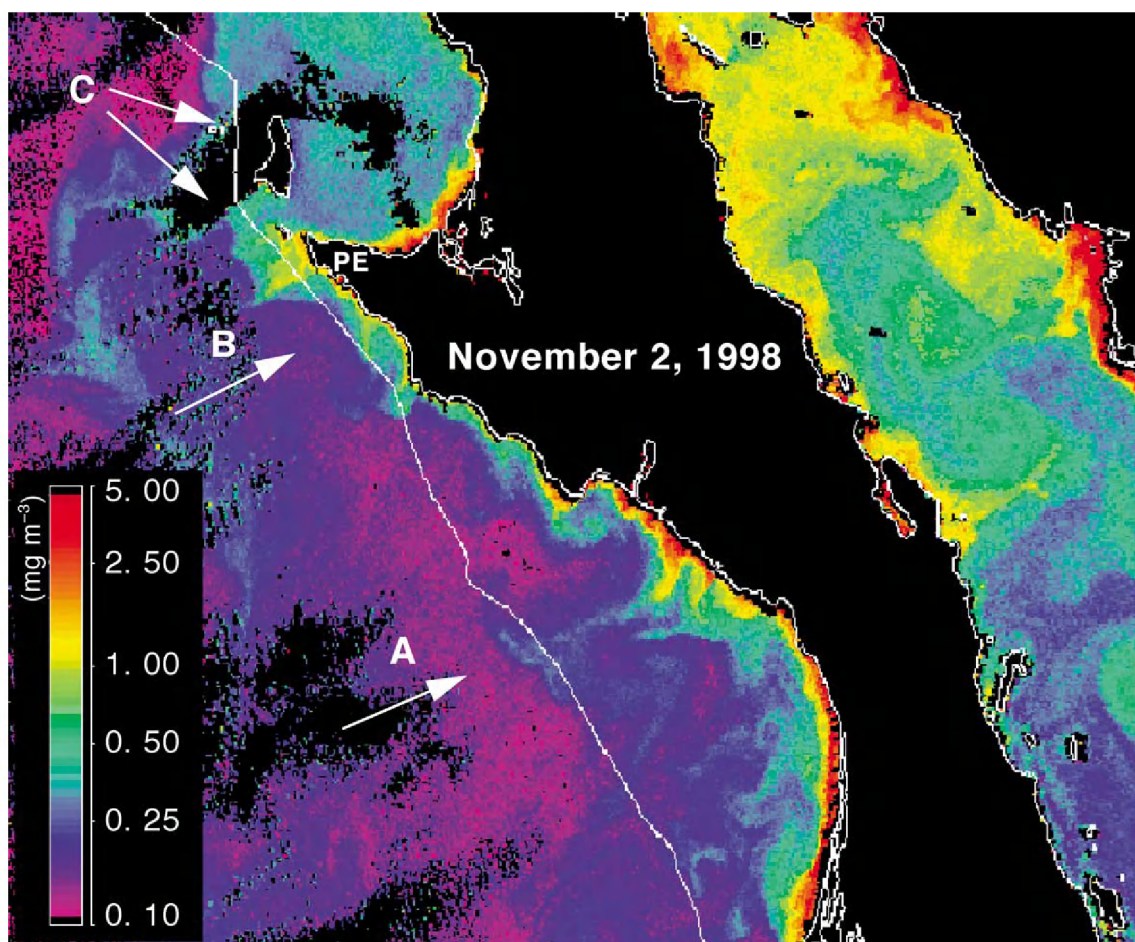


Fig. 5. SeaWiFS ocean color image of chlorophyll for November 2, 1998. Ship track (white line) shows position of *R/V Revelle* during northward transit on November 2, 1998, similar to previous figure. Arrow A shows dissipating eddy; arrow B shows three eddies of high chlorophyll; arrows C shows areas of Ba-depleted surface water.

temperature and salinity data (Fig. 3), provide evidence for pronounced filaments and eddies off coastal promontories (Figs. 4 and 5, arrows A and B). Some eddies, such as those near Punta Eugenia between 27°N and 28°N, were due to upwelling of colder, less saline Pacific Intermediate water (Bakun and Nelson, 1977; Bakun, 1990; Hickey, 1998). Fortuitously, the ship surveyed close to the coast (Fig. 1) south of Punta Eugenia (27–28°N). Sharp and correlated changes in temperature (3 °C), FDOM, chlorophyll, and nutrients were indicative of nearshore upwelling and increased biological productivity (Figs. 3–5).

Though upwelling is usually strongest in spring and summer, Figs. 4 and 5 show that there were visible filaments of biologically productive waters around promontories like Punta Eugenia and Cabo San Lazaro, and west of Isla Cedros (28°N). Coastal upwelling and surface eddies produced thin filaments of cold water enriched in organic matter, chlorophyll, and silica, and bounded by pronounced density fronts (Fig. 3). These filaments and eddies were more pronounced on October 31, 1998 (Fig. 4A–B) than several days later on November 2, 1998 (Fig. 5A–B). Nevertheless, both SeaWIFS imagery and shipboard hydrographic data show clearly filaments of cold, nutrient-rich surface waters coincident with increased biological activity between 27°N and 28°N on November 2, 1998 when the *R/V Revelle* transited through this area.

3.3. Radioisotope tracer

Radiocesium (^{137}Cs) behaves as a conservative element in seawater, similar to other alkali metal ions. It has a half-life of 30.2 years, and persists in the environment from previous atmospheric nuclear testing, and from nuclear power and processing facility discharge. Radiocesium provides important age information for characterizing upper ocean water circulation, because its half-life is short compared with the time scale of ocean circulation and mixing. Combined with in situ water density (sigma- θ) data, it provides additional constraint for upwelling of Pacific Intermediate water along the Baja coastal margin.

There are few hydrographic and ^{137}Cs data showing lateral and vertical distribution offshore Baja. During

this survey (Fig. 1), we measured ^{137}Cs in surface water from San Diego to the Gulf of California (Volpe et al., 2002). Surface water between Punta Eugenia and Cabo San Lazaro had low ^{137}Cs activity (0.85–1.07 mBq/l) and high sigma- θ (23.62–23.75) compared with surface water in the California Current (2.33–2.44 mBq/l, 23.82–23.91) and the Gulf of California (1.44–1.55 mBq/l, 21.85–21.90) (Volpe et al., 2002). Radiocesium activity levels in surface water south of Punta Eugenia are two to three times lower than California Current surface water off the Baja coast. Previous vertical profiles of ^{137}Cs activity taken in the North Pacific during GEOSECS (stations 201, 347), the Farallons, and Santa Monica Basin (Noshkin et al., 1978; Bowen et al., 1980; Livingston et al., 1985; Wong et al., 1992) showed ^{137}Cs decreasing with depth. Activity levels decreased to method detection limits by 400–600-m depths, which indicated that ^{137}Cs was mostly confined to the mixed layer in the upper surface above the thermocline. Therefore, Pacific Intermediate water is characterized by little or no ^{137}Cs activity, because it has been isolated both from initial fallout on the ocean surface and subsequent runoff from land. The radiocesium data are corroborative evidence with hydrographic (in-situ water density) and SeaWIFS imagery (chlorophyll *a*) for lateral offshore transport of California Current surface water, which was replaced by upwelling of deeper, nutrient-rich Pacific Intermediate water.

3.4. Biological activity

Fig. 6 shows the positive correlation between increasing chlorophyll and FDOM in surface water off Baja California between 24.91°N and 28.81°N, on November 2, 1998. There are three separate trends evident in Fig. 6 that correspond to chlorophyll and FDOM enrichment of varying degree. One trend (26.07°N) was characterized by high FDOM (0.17 $\mu\text{g/l}$) and low chlorophyll (<0.02 $\mu\text{g/l}$). These data delineate a large filament seen on satellite imagery that extended westward offshore between 25.2°N and 26.1°N (Figs. 4 and 5, arrow A). Relatively low chlorophyll observed shipboard is consistent with the SeaWIFS chlorophyll *a* observation on November 2, which showed reduced biological activity (from 0.7 to 0.3 mg/m^3) over several days. This trend of high FDOM and rela-

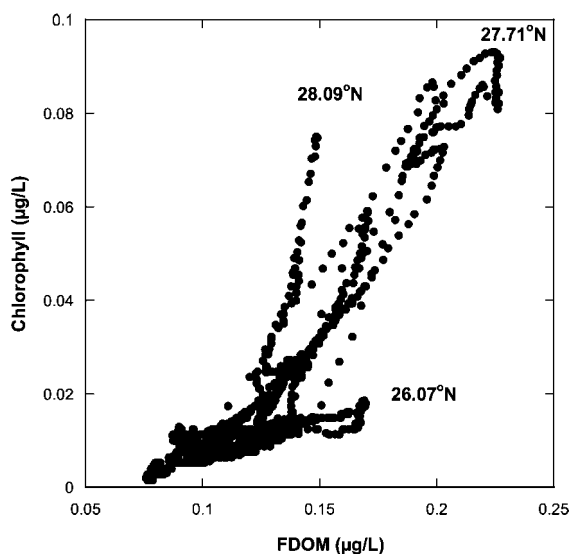


Fig. 6. Plot of chlorophyll ($\mu\text{g/l}$) versus FDOM ($\mu\text{g/l}$) in surface waters off Baja California between 24.91°N and 28.81°N (November 2, 1998). Geographic coordinates correspond to maxima or minima shown on Fig. 3.

tively low chlorophyll is correlated with waning phytoplankton activity.

A second trend (27.71°N) showed positively correlated chlorophyll and FDOM between 27.1°N and 27.7°N (Fig. 6). Shipboard measurements of three distinct peaks in chlorophyll and FDOM concentration (Fig. 3) coincided with three filaments of relatively high chlorophyll concentration ($>1 \text{ mg/m}^3$), which are evident in the November 2 SeaWiFS image (Fig. 5, arrow B). These filaments were less pronounced on the October 31 SeaWiFS image (Fig. 4), suggesting that the increase in phytoplankton activity observed in this area developed over a short period ($< \text{two days}$). Surface waters exhibiting positively correlated chlorophyll and FDOM trends (e.g., 27.71°N) are also characterized by relatively recent increases in phytoplankton activity (SeaWiFS).

There is a third trend (28.09°N) of chlorophyll increasing relative to FDOM (Fig. 6) due west of Isla Cedros, where the ship changed course from northwesterly to northward (Fig. 1). Though the cloud cover west of Isla Cedros partially obscured the SeaWiFS image for November 2, 1998 (Fig. 5), the ship track crossed an area that exhibited high chloro-

phyll *a* concentrations 2 days earlier on October 31 (Fig. 4). This trend of markedly increasing chlorophyll relative to FDOM may indicate a very recent increase in phytoplankton activity associated with upwelling of cold nutrient-rich water.

3.5. Barium and biological activity

Between these areas of increased biological activity and elevated chlorophyll concentration, there was significant depletion of nearly 65% in surface water Ba off Punta Eugenia (28°N) (Esser and Volpe, in press (a); Volpe et al., 2001). This Ba depletion occurred over a distance of nearly 25 km, from 27.8°N to 28.0°N , where the ship changed to a northward course west of Isla Cedros (Fig. 5, arrows C). These surface waters had relatively warm temperature, and low chlorophyll, FDOM, and silicic acid (Fig. 3). Consecutive SeaWiFS images suggest that surface water chlorophyll *a* is increasing to the south and dissipating to the north of this area (Figs. 4 and 5). There was another locality that showed surface water Ba depletion of 25% between 28.1°N and 28.4°N , due west of Isla Cedros (Fig. 5, arrows C).

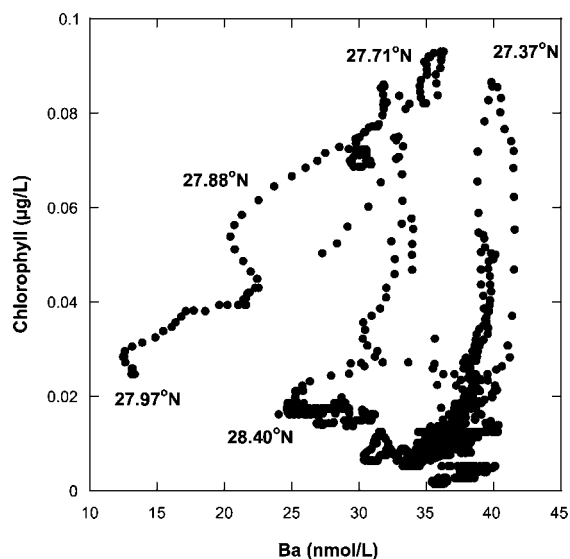


Fig. 7. Plot of chlorophyll ($\mu\text{g/l}$) versus Ba (nmol/l) content in surface waters off Baja California (same as Fig. 6).

Besides the two areas that showed Ba, chlorophyll, FDOM, and silicic acid depletion in surface water, there was little correlation between Ba and chlorophyll (Fig. 7), Ba and salinity or temperature (Fig. 8), and Ba and silicic acid (Fig. 9). Dissolved Ba was between 35 and 39 nmol/l, which is consistent with GEOSECS data for North Pacific surface water (Bender et al., 1972; Broecker and Peng, 1982). Salinity and temperature values ranged from 33.5 to 34.5 and 17 to 24 °C, respectively. In comparison, Ba- and chlorophyll-depleted surface waters near 27.97°N and 24.80°N were relatively cold (17.5–19.0 °C) and less saline (33.5–33.7). In situ water density values ranged between 23.4 and 24.3, while Ba-depleted surface waters had intermediate sigma-t values (23.85–23.95), and silicic acid was at the low end of the observed values (<1 μmol/l).

Typically, barium distribution shows relative enrichment as water depth increases, with maximum values beneath the upper mixed layer (Chan et al.,

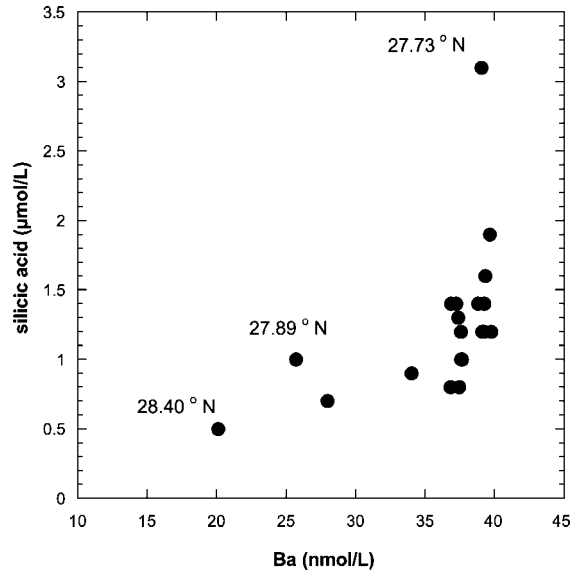


Fig. 9. Plot of silicic acid (μmol/l) versus Ba (nmol/l) in bottle samples taken off Baja California (same as Fig. 6).

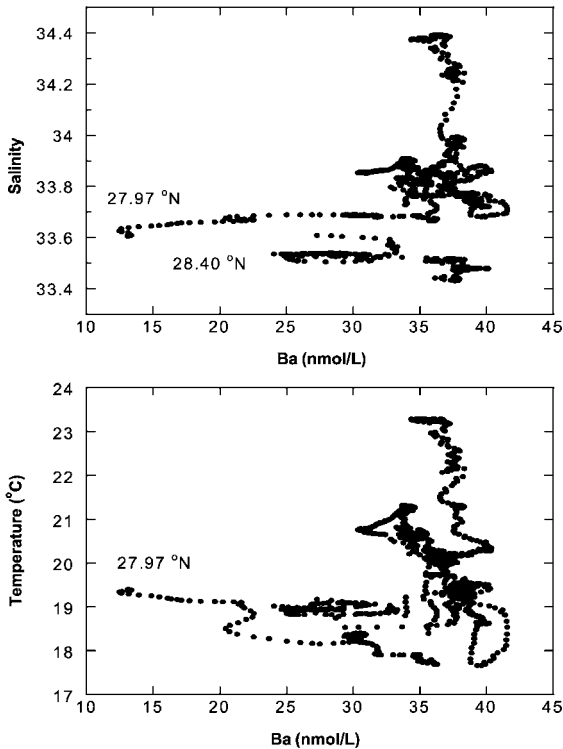


Fig. 8. Plots of salinity and temperature versus Ba (nmol/l) in surface waters off Baja California (same as Fig. 6).

1977; Östlund et al., 1987). Other processes that control Ba distribution, such as mixing with deep or coastal waters, or upwelling of nutrient-rich deep water, like that observed near Punta Eugenia, lead to enhanced, not depleted surface concentrations of dissolved Ba. River runoff typically elevates coastal Ba concentrations (Falkner et al., 1994; Shaw, 1999), however, freshwater flow into the Pacific Baja coast is negligible. The observed Ba depletion in surface waters near Punta Eugenia can be explained by elevated biological productivity in surface waters, which led to barite precipitation, or possibly by uptake of Ba by phytoplankton (Esser and Volpe, in press (a)).

Recent studies suggest that acantharians, which are protists that secrete celestite, may play an important role in the marine chemistry of Ba and Sr (Bernstein et al., 1992, 1998). The lateral offset between silicic acid and chlorophyll maxima and the Ba minima argues against active Ba uptake by phytoplankton, such as acantharia. There was little supporting chemical evidence for acantharian (celestite) removal, since strontium concentrations, which were measured by isotope dilution ICPMS in the bottle samples returned to the lab, were

uniform (Sr/salinity ratio varied by less than 0.5%) for these strongly Ba-depleted surface waters (Esser and Volpe, in press (a)). Barium removal associated with biological productivity (Bishop, 1988; Dehairs et al., 1991; Stroobants et al., 1991) is the most consistent explanation for the observed Ba depletion in surface waters near Punta Eugenia (Esser and Volpe, in press (a)).

The frontal zone across which the Ba minima occurs probably reflects the waning stage of a bloom, in which nutrients were depleted, and phytoplankton were no longer abundant. In this case, dying phytoplankton and zooplankton fecal material provided an environment for the precipitation and export of marine barite from productive surface water to seafloor sediments. It seems that the Punta Eugenia Ba depletion zone was on the northern edge of an upwelling event (Figs. 4 and 5). If so, then the Ba, hydrographic, and satellite data suggest that Ba removal due to biological activity is a relatively rapid phenomenon, which occurs over a period measured in days.

In contrast, satellite imagery indicates reduced phytoplankton activity in several areas (i.e., 26.07°N) over 2 days with little indication of any anomalous depleted Ba concentration in surface water (Fig. 3). Thus, for reasons not yet understood, post bloom waters may not always result in reduction of dissolved Ba concentrations. On the other hand, it may be that Ba removal occurred beneath the sampling depth of the bow intake on the *Revelle*. In this instance, a vertical cast would have been informative.

The dissolved Ba deficit in the depletion zone corresponds to removal of particulate Ba of approximately 19 nmol/kg (Esser and Volpe, in press (a)). This is a factor of 2 higher than particulate Ba concentrations of 9 nmol/kg observed in productive surface waters of the southern ocean (Dehairs et al., 1997). Integrating the deficit over a vertical column of 10 m, and assuming the monthly averaged Ba removal from this water mass was dominated by this transient event yields a monthly averaged Ba export rate of 200 nmol/cm²/year. This flux is three times higher than monthly averaged Ba fluxes of 60–80 nmol/cm²/year, which were determined from sediment trap data in the Atlantic and Pacific (Dymond et al., 1992; Dymond and Collier, 1996; Fagel et al., 1999; Dehairs et al., 2000). The Ba depletion events at 28.0°N and 28.4°N

seem to occur in discrete areas and last for a short time. Sediment traps set at depths of 600 to 3500 m would average these transient events over the collection interval, and may miss confined events. Moreover, if mixing between particulates in adjacent water masses (i.e., advection) occurs during settling, then sediment traps will record a spatially averaged signal. Both effects would dampen surface peak flux. This is another instance where vertical casts would be informative. Nevertheless, deployment of an integrated analytical observation system provides a means to observe short-term effects of ocean productivity phenomena.

The hydrographic, trace element, radiocesium, and satellite SeaWiFS data constrain physical ocean models, which suggest that biological productivity and upwelling off Baja promontories is a highly fluctuating process in time and space. In recent years, barium has been used to investigate changes in ocean circulation, upwelling conditions, and surface water productivity over a variety of time scales, and to measure net export of carbon from the euphotic zone (Falkner et al., 1993). This unexpected variability in dissolved Ba illustrates that even for elements with well-known distributions, the coastal ocean is grossly undersampled (Johnson et al., 1992), and that solid-phase Ba can serve as a proxy for modern and paleo-ocean productivity (Esser and Volpe, in press (a)).

4. San Diego Bay: seaward chemical flux and coastal productivity

High population density along the Southern California coastline has a significant effect on water quality along the coastal margin. There have been previous studies of trace metal distribution in San Diego Bay (Zirino et al., 1978, 1998; Flegal and Sañudo-Wilhelmy, 1993), the adjacent coastal areas (Sanudo-Wilhelmy and Flegal, 1991, 1992, 1994, 1996), and even some research linking chemical contamination and biological toxicity (McCain et al., 1992). Recently, several studies describe physical exchange between San Diego Bay and the coastal ocean, which is dominated by tidal pumping during ebb (tidal jet) and flood (tidal sink) cycles (Chadwick and Largier, 1999a,b). These investiga-

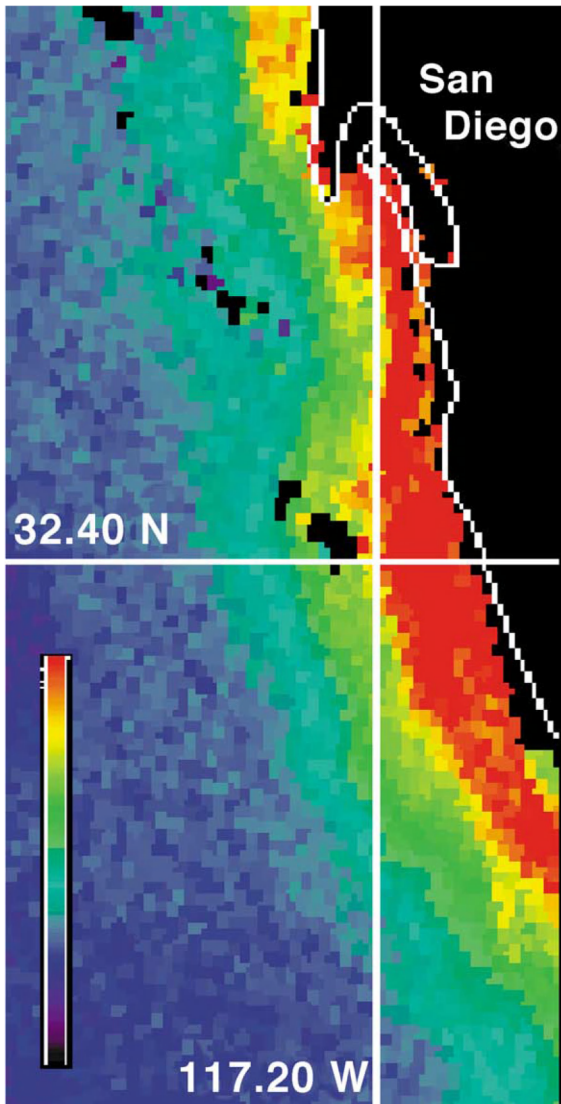


Fig. 10. SeaWiFS ocean color image for San Diego Bight on September 11, 1999 (S1999254195708_L2_chla). Chlorophyll concentration varies from less than 0.10 to 5 mg/m³.

tors used flow measurements and a dissolved organic UV fluorescent tracer to model the tidal pumping process, and quantify exchange between the bay and ocean. Still, the fate and dispersal of chemical plumes from San Diego Bay as well as Mission Bay and the Tijuana River have been little studied.

These plumes are the primary mechanism for exchange and transfer of nutrients, biological organ-

isms, and trace metals between the bays and the coastal ocean. Important parameters include the rates of exchange of nutrients and trace metals in mixed waters, the effects of these trace metals on biological productivity, and the short-term fate of dissolved and particulate material flushing from the bays. A first step in understanding these aspects of coastal biogeochemical processes is to quantify the distribution, both temporal and spatial, of biological and chemical species. The main purpose of this survey was to use the at-sea ICPMS to quantify trace metal composition of waters in the San Diego coastal zone in conjunction with simultaneous sampling of invertebrate larvae (L. Levin, SIO). In the future, continued high-resolution water chemistry measurements will permit full characterization of the spatial variation (within bay, bay vs. coastal) and temporal shifts (within the tidal cycle) in elemental signatures.

4.1. Satellite observation

SeaWiFS chlorophyll *a* concentrations in San Diego coastal water for September 11, 1999 are

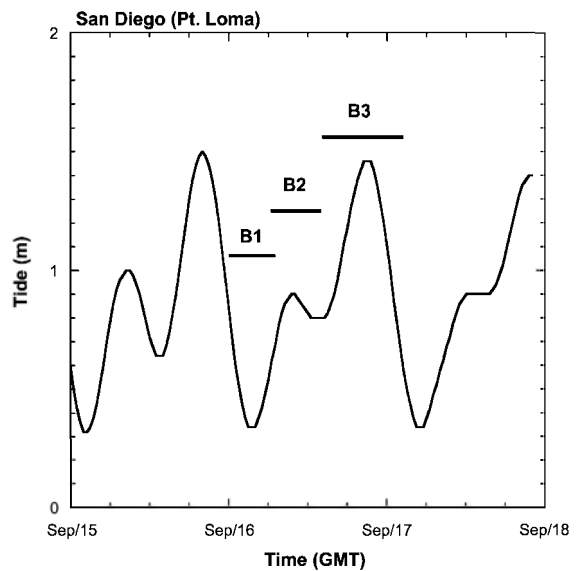


Fig. 11. Tidal range (m) versus time (GMT) for San Diego during the survey. Periods for legs B1, B2 and B3 are shown.

shown in Fig. 10. Surface waters with high chlorophyll concentrations, greater than 5 mg/m^3 , were confined to a 10-km-wide zone that extended longshore from the San Diego Bay entrance to the southern end of the image, near Ensenada, Mexico. To the north, beyond the image boundary, there was a chlorophyll *a* enriched filament that extended longshore southward from Long Beach into the

Santa Monica Basin. There were several large eddies with chlorophyll *a* concentrations up to 1.0 mg/m^3 in the Santa Monica Basin. Surface waters due west of San Diego had uniformly low chlorophyll *a* less than 0.2 mg/m^3 . The image resolution is approximately 1 km, and it provides an overview of the spatial distribution of chlorophyll *a* along the Southern California coast. However, ocean surface

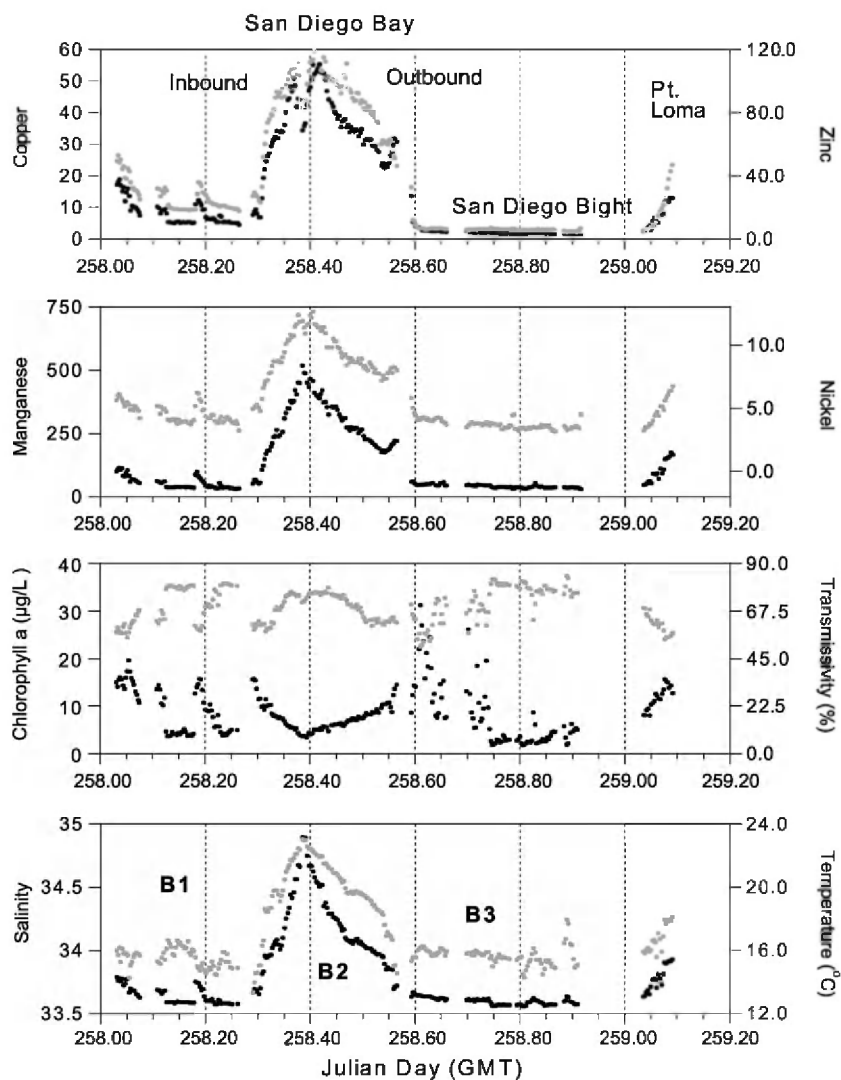


Fig. 12. Oceanographic and trace element data from the September 1999 cruise aboard the *R/V Sprout* in San Diego Bay (B2) and the adjacent coastal ocean (B1, B3). Times are in Julian Days (GMT). Panel 1: Cu (nmol/l), dark circles; Zn (nmol/l), gray circles. Panel 2: Mn (nmol/l), dark circles; Ni (nmol/l), gray circles. Panel 3: Chlorophyll ($\mu\text{g/l}$), dark line; light transmissivity (%), gray line. Panel 4: Salinity, black line; temperature ($^{\circ}\text{C}$), gray line.

radiance is more complicated in coastal areas (Case II waters) than in deep ocean, and the image provides little information that elucidates either San Diego Bay chlorophyll *a* distribution, or dispersal of Bay waters in the coastal ocean.

4.2. Hydrography

The San Diego coastal margin survey consisted of sequential segments corresponding to B1, B2, and B3 in Fig. 2. Survey B1 was conducted around the entrance to San Diego Bay offshore Pt. Loma during low slack tide (Fig. 11). Depth of the tow body varied between 2.1 and 2.5 m. This survey was conducted to establish a baseline for delineating the tidal jet as it entered the coastal ocean during ebb flow. It coincided with the study area of previous research that examined tidal exchange between San Diego Bay and the coastal ocean (Chadwick and Largier, 1999a,b). The next survey leg was a continuous sampling loop of San Diego Bay from outside the entrance through the outer bay to the 24th Street Marine Terminal and inner bay, and then back to the entrance (Fig. 2, B2). The survey began outside the bay with the onset of

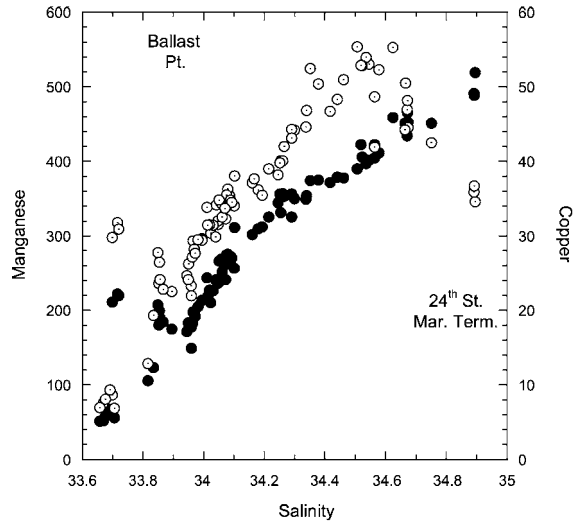


Fig. 14. Mn (nmol/l), closed circles, and Cu (nmol/l), open circles versus salinity for surface water in San Diego Bay (survey B2).

flood tide (Fig. 11), and ended near the starting point on slack tide. On the transit into the bay, the tow body depth was 2.35 ± 0.05 m, and 1.34 ± 0.04 m on the return transit. The last survey was conducted along shore and across the San

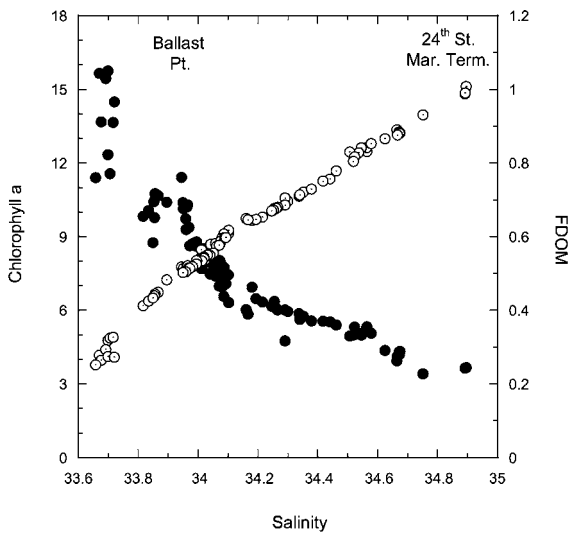


Fig. 13. Chlorophyll ($\mu\text{g/l}$), closed circles and FDOM ($\mu\text{g/L}$), open circles versus salinity for surface water in San Diego Bay (survey B2).

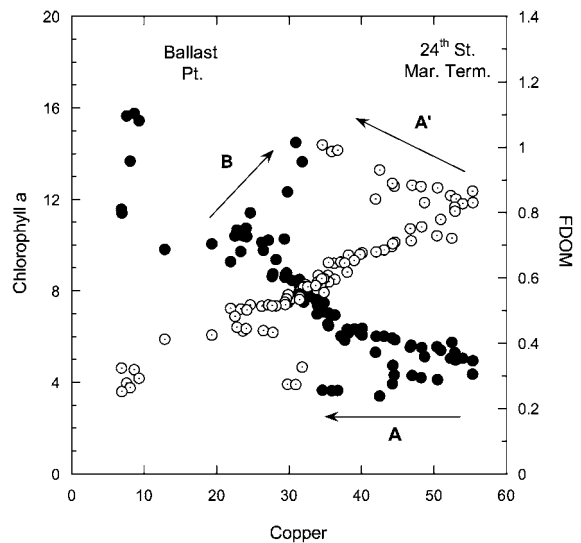


Fig. 15. Chlorophyll ($\mu\text{g/l}$), closed circles, and FDOM ($\mu\text{g/L}$), open circles versus Cu (nmol/l) for surface water in San Diego Bay (survey B2).

Diego Bight (Fig. 2, B3), during high slack tide (Fig. 11). Tow body depth varied between 2.2 and 3.1 m. The purpose was to establish the limits of the San Diego Bay tidal jet as it dispersed into the Bight.

4.3. San Diego Bay and trace metals

Trace metal and sensor data show that San Diego Bay was enriched in Mn, Ni, Cu, Zn, Cd, and FDOM with respect to the coastal ocean (Fig. 12). Salinity, temperature, FDOM, and trace metals

show increasing gradients from the entrance and outer bay to the inner bay (Fig. 12, Cd is not shown). Chlorophyll shows monotonic decreasing values with increasing temperature and salinity through the bay (Figs. 12 and 13). The strong inverse correlation between chlorophyll and light transmissivity in San Diego Bay and the adjacent coastal surface water suggests that biomass (represented by chlorophyll) was the principal component degrading water clarity (Fig. 12, panel 3). San Diego Bay is a semi-enclosed embayment with little river input at this time of the year.

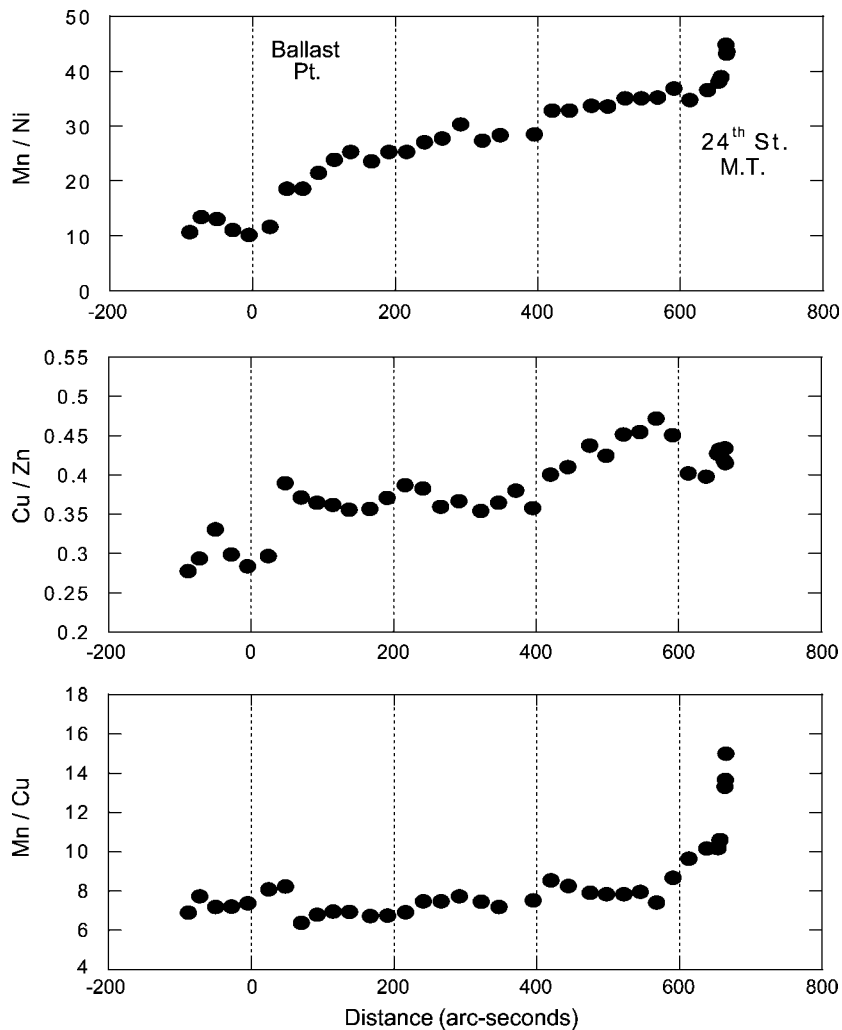


Fig. 16. Plots of Mn/Ni, Cu/Zn and Mn/Cu for the inbound portion of B2 San Diego Bay survey versus distance (arc-seconds). Distance is calculated from the center of the shipping channel west of the tip of Pt. Loma, with positive distance being into the Bay.

Though nonlinear, there is strong correlation between chlorophyll and salinity, and FDOM and salinity in San Diego Bay water (Fig. 13). Chlorophyll decreases rapidly from outside the bay entrance to Ballast Point, and then gradually from the outer bay to south bay. FDOM increases uniformly with salinity (Fig. 13). The inverse relation between chlorophyll and FDOM is striking compared with the strong positive correlation seen in productive surface waters offshore Baja California (Fig. 6). Previous investigation noted a strong ultraviolet fluorescence gradient in the outer bay of approximately $3 \mu\text{g l}^{-1} \text{ km}^{-1}$ that was associated with leaching of polycyclic aromatic hydrocarbons from creosote saturated pier structures (Chadwick and Largier, 1999b). The values of FDOM in this study are lower than in the previous study, but the emission wavelength of the UV-fluorometer (440 nm) in this study is different than that typically used to investigate hydrocarbons (360 nm).

Both Mn and Cu show uniformly increasing concentration with salinity and distance into the bay (Fig. 14). Zinc, Ni, and Cd show similar positive trends. However, there was markedly different surface water near the southern end of the 24th Street Marine Terminal, where the inbound transit ended. At this location in the south bay, temperature (23°C), salinity (34.89), FDOM ($1.0 \mu\text{g/l}$), and Mn (519 nmol/l) were at maxima, while Cu, Zn, and Ni concentrations fell 45%, 30%, and 10%, respectively. The sudden decrease in Cu was uncorrelated with change in chlorophyll concentration, which was already at the minima ($4 \mu\text{g/l}$) for the survey (Fig. 15—trend A). In contrast, FDOM increased while Cu decreased across this surface water front (Fig. 15, trend A'). On the return transit, surface water near the bay entrance had elevated chlorophyll ($10\text{--}14 \mu\text{g/l}$) with little change in Cu ($25\text{--}35 \text{ nmol/l}$) (Fig. 15 trend B). Similar trends were observed for the other trace metals at the bay entrance, which suggests tidal mixing of bay water and “new” coastal water.

Trace element ratios of surface water on the inbound leg of the B2 transit are shown in Fig. 16. Distance was calculated in units of arc-seconds from a reference point in the center of the shipping channel west of the tip of Pt. Loma (32.67°N , 117.23°W). Locations for Ballast Point and the 24th Street Marine Terminal are +73 and +650

arc-seconds, respectively. Mn/Ni (11–12) and Cu/Zn (0.3) ratios of tidally mixed bay and coastal water are low compared with bay water (Fig. 16). The ratio of Mn to Ni increases smoothly from Ballast Point (Mn/Ni=20) to the south bay (600 arc-sec: Mn/Ni=37), and then it sharply increases (Mn/Ni=45) near the 24th Street Marine Terminal. Cu/Zn ratios are uniform (0.37) between Ballast Point and downtown San Diego (400 arc-seconds), where the ratio increases toward the 24th Street Marine Terminal (Cu/Zn=0.47), and then it sharply decreases (Fig. 16). Mn/Cu ratios of surface water are somewhat uniform through outer bay to south (Mn/Cu=7–9), and then the ratio increases substantially near the southern terminus of the survey due to relatively high Mn and low Cu.

There are distinct changes in trace metal concentrations and ratios near the 24th Street Marine Terminal that probably reflect differences between main channel surface water that is controlled by tidal mixing, and water from the shallow southern portion of the bay. Elevated levels of Ni (and probably Mn and Cd) have been attributed to sediment and pore water diagenetic processes in South San Diego Bay (Flegal and Sañudo-Wilhelmy, 1993). Since Ni, Mn, and Cd are linearly correlated, elevated Mn and Cd mostly like reflects

Table 1
San Diego Bay chemical gradient and flux

Ballast Point-24th Street Marine Terminal			
	Transit in (24-m depth)	Transit out (1.4-m depth)	Flux into coastal ocean
MN	18	– 16	200–440
Ni	0.29	– 0.26	11–17
Cu	1.7	– 1.7	27–78
Zn	2.8	– 2.8	120–200
Cd	12	– 21	3
Chlorophyll	– 0.40	0.28	
FDOM	0.021	– 0.022	20
Temperature	0.26	– 0.23	
Salinity	0.041	– 0.041	

Chlorophyll and FDOM are in $\mu\text{g l}^{-1} \text{ km}^{-1}$; trace metal concentrations in $\text{nmol l}^{-1} \text{ km}^{-1}$, except Cd, which is in $\text{pmol l}^{-1} \text{ km}^{-1}$; temperature in $^\circ\text{C km}^{-1}$; and salinity in km^{-1} . Negative values represent decreasing concentration with distance. Chemical fluxes are in units of kilogram per average tidal prism.

input from sediments in the south. In contrast, Cu and Zn concentrations reach maxima at lower salinity (Fig. 14), and Cu/Zn ratios increase between downtown San Diego and the 24th Street Marine Terminal (Fig. 16). These changes may indicate a near-point source in this region that is not totally dispersed by tidal mixing. The decrease in Cu and Zn concentrations and Cu/Zn ratios with increasing salinity and FDOM to the south may reflect selective removal on suspended organic-rich material.

Table 1 summarizes chemical gradients of dissolved constituents and chlorophyll in San Diego between

Ballast Point and the 24th Street Marine Terminal. Changes in the chemical parameters varied two- to threefold and were well correlated ($r^2 > 0.9$) with distance. The inbound and outbound gradients of each constituent were the same, with several minor exceptions. The gradients for Mn (18 vs. 16 $\text{nmol l}^{-1} \text{km}^{-1}$) and chlorophyll (0.40 vs. 0.28 $\mu\text{g l}^{-1} \text{km}^{-1}$) reflect minor differences in surface water near Ballast Point on flood (inbound) versus slack (outbound) tide. Previous work estimated that approximately one half of the water entering the bay on a flood tide is “new” coastal ocean water, and one half is bay water that was discharged on the ebb tide (Chadwick and Largier, 1999a).

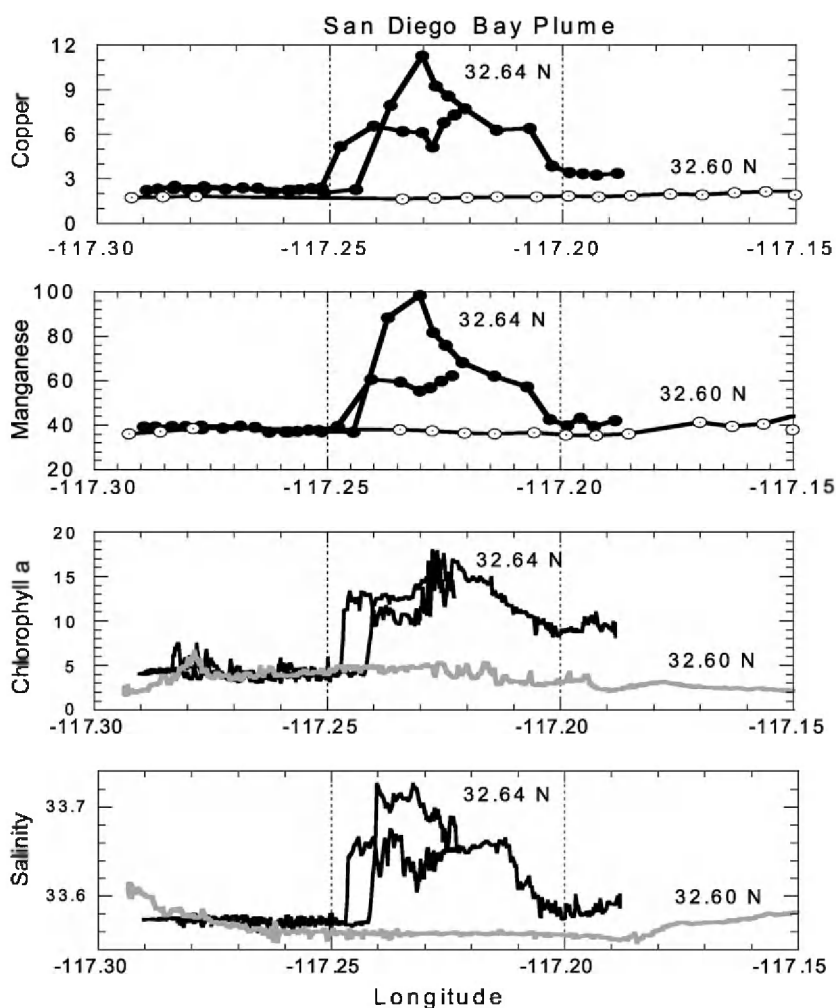


Fig. 17. Plots of Cu (nmol/l), Mn (nmol/l), chlorophyll ($\mu\text{g/l}$) and salinity along east–west transects in the coastal ocean adjacent to the mouth of San Diego Bay: B1 survey along 32.64°N, dark line and closed symbols; and B2 survey along 32.60°N, gray line and open symbols.

4.4. San Diego Bay plume

The trace metal enrichment patterns can be used to tag tidal jet Bay water as it enters the San Diego Bight (segments B1 and B3). Fig. 17 shows detailed plots of trace metal enriched water along the 32.64°N (B1) and 32.60°N (B3) transects. The first transect is approximately 3.3 km south of the bay entrance, and the other is 7.8 km south. The San Diego Bay tidal jet plume is evident in elevated Mn (100 nmol/l) and Cu (10 nmol/l), as well as Ni, Zn, Cd, and FDOM abundance along the 32.64°N transect (Fig. 17). Elevated chlorophyll and salinity are also characteristic of the plume signature. It is undetermined where the chlorophyll increase occurs, since this is atypical of inner San Diego Bay water. The trace metal concentrations along this transect are approximately half those in surface water inside the bay, near Ballast Point. The survey segment along 32.60°N is noteworthy in that the trace metal enriched Bay plume is not evident in San Diego Bight 8 km south of the bay entrance. This is consistent with calculations showing the tidal jet extending approximately 4.3 km beyond the mouth of the bay for an average tidal range of 1.4 m (Chadwick and Largier, 1999b).

It is possible to estimate the flux of trace metals from San Diego Bay given the gradients, tidal plume concentration in excess of coastal water, and an average tidal prism volume of about $5.5 \times 10^7 \text{ m}^3$ (Chadwick and Largier, 1999b). Table 1 shows a range for the trace metals based on concentrations observed near the mouth of bay (e.g., what is available) and in the tidal jet offshore (e.g., what escapes). Manganese (200–400 kg) and Zn (120–200 kg) are the principal metals discharged from the bay, though Cu (27–78 kg) may be underestimated depending on the fraction sequestered with organic compounds.

5. Conclusions

We described a new ocean observation system integrating mass spectroscopy, hydrographic instrumentation, and satellite imagery. We have shown that a mass spectrometer can be successfully taken to sea without deleterious effect, and used to rapidly determine trace metals in seawater for many days. This permits mapping of important biologically influenced

elements, such as Ba, at high spatial resolution over a regional scale. We extended this capability to a wider range of biologically active trace elements (Mn, Ni, Cu, Zn, and Cd) that are present at very low concentrations, and effected by seawater matrix interference, which required on-line pre-concentration and matrix elimination. The combination of field-based instrumentation, parts per 10^{12} detection limit, and rapid analytical cycling allowed mapping of trace metals in the coastal environment at spatial resolutions previously unachievable. In the future, this type of system will dramatically increase our understanding of the distribution and geochemistry of these metals, and of near-shore ocean biology and productivity. Applications include mapping pollutant flux at critical interfaces (bay–ocean) over tidal cycles that vary in intensity, observing the regional effect of extreme discharge due to storms and river runoff, and correlating trace metal distribution with biological diversity and productivity.

Acknowledgements

The authors thank D. Macdougall, J. Hawkins, and P. Lonsdale at SIO for access to ship time aboard the *Revelle*; C. Mahn and J. Gieskes at SIO for keeping the San Diego Bay experiment afloat; and B. Wilson and the SIO shipboard group for support. Denis Nadeau and Jim Acker at NASA/GSFC graciously processed and supplied SeaWiFS images based on data acquired from the Monterey Bay Aquarium Research Institute HRPT station. Several patient reviewers made constructive suggestions that significantly improved the manuscript. This research was funded by a Laboratory Directed Research and Development grant (99-ERD-064), and WFO Project L-4401. The work was performed under the auspices of the US Department of Energy by the University of California, Lawrence Livermore National Lab under contract W-7405-Eng-48.

References

- Abdullah, M.I., El-Rayis, O.A., Riley, J.P., 1976. Re-assessment of chelating ion-exchange resins for trace metal analysis of sea water. *Analytica Chimica Acta* 84, 363–368.
- Bakun, A., 1990. Global climate change and intensification of coastal ocean upwelling. *Science* 247 (4939), 198–201.

- Bakun, A., Nelson, C.S., 1977. Climatology of upwelling related processes off Baja California. California Cooperative Oceanic Fisheries Investigations Report XIX, 107–127.
- Bandong, B.B., Volpe, A.M., Esser, B.K., Bianchini, G.M., 2001. Pre-concentration and measurement of low levels of gamma-ray emitting radioisotopes in coastal waters. *Applied Radiation and Isotopes* 55 (5), 653–665.
- Bender, M., Snead, T., Chen, L., Bacon, M.P., Edmond, J.M., 1972. Barium intercalibration at Geosecs I and III. *Earth and Planetary Science Letters* 16, 81.
- Bernstein, R.E., Byrne, R.H., Betzer, P.R., Greco, A.M., 1992. Morphologies and transformations of celestite in seawater: the role of acantharians in strontium and barium geochemistry. *Geochimica et Cosmochimica Acta* 56 (8), 3273–3279.
- Bernstein, R.E., Byrne, R.H., Schijf, J., 1998. Acantharians: a missing link in the oceanic biogeochemistry of barium. *Deep-Sea Research. Part 1. Oceanographic Research Papers* 45 (2–3), 491–505.
- Bishop, J.K.B., 1988. The barite–opal–organic carbon association in oceanic particulate matter. *Nature* 332, 341–343.
- Bloxham, M.J., Hill, S.J., Worsfold, P.J., 1994. Determination of trace metals in sea-water and the on-line removal of matrix interferences by flow injection with inductively coupled plasma mass spectrometric detection. *Journal of Analytical Atomic Spectrometry* 9 (9), 935–938.
- Bowen, V.T., Noshkin, V.E., Livingston, H.D., Volchok, H.L., 1980. Fallout radionuclides in the Pacific Ocean: vertical and horizontal distributions largely from GEOSECS stations. *Earth and Planetary Science Letters* 49, 41–434.
- Boyd, P.W., Law, C.S., 2001. The Southern Ocean Iron Release Experiment (SOIREE)—introduction and summary. *Deep-Sea Research. Part 2. Topical Studies in Oceanography* 48 (11–12), 2425–2438.
- Bray, N.A., 1988. Thermohaline circulation in the Gulf of California. *Journal of Geophysical Research* 93 (C5), 4993–5020.
- Broecker, W.S., Peng, T.-H., 1982. Tracers in the Sea. Lamont–Doherty Geological Observatory, Palisades, NY.
- Bruland, K.W., Franks, R.P., Knauer, G.A., Martin, J.H., 1979. Sampling and analytical methods for the determination of copper, cadmium, zinc and nickel at the nanogram per liter level in sea water. *Analytica Chimica Acta* 105, 233–245.
- Butler, A., 1998. Acquisition and utilization of transition metal ions by marine organisms. *Science* 281 (5374), 207–210.
- Chadwick, D.B., Largier, J.L., 1999a. The influence of tidal range on the exchange between San Diego Bay and the ocean. *Journal of Geophysical Research, [Oceans]* 104 (C12), 29885–29899.
- Chadwick, D.B., Largier, J.L., 1999b. Tidal exchange at the bay–ocean boundary. *Journal of Geophysical Research, [Oceans]* 104 (C12), 29901–29924.
- Chan, L.H., Drummond, D., Edmond, J.M., Grant, B., 1977. On the barium data from the Atlantic GEOSECS Expedition. *Deep-Sea Research* 24, 613–649.
- Coale, K.H., Bruland, K.W., 1988. Copper complexation in the northeast Pacific. *Limnology and Oceanography* 33, 1084–1101.
- Coale, K.H., Bruland, K.W., 1990. Spatial and temporal variability in copper complexation in the North Pacific. *Deep-Sea Research. Part A, Oceanographic Research Papers* 37 (2), 317–336.
- DeCarlo, E.H., Resing, J.A., 1998. Determination of picomolar concentrations of trace elements in high salinity fluids by FIA-ICP-MS (abstr.). Winter Conference on Plasma Spectrochemistry. ICP Information Newsletter, Scottsdale, AZ, pp. 82–83.
- Dehairs, F., Stroobants, N., Goeyens, L., 1991. Suspended barite as a tracer of biological activity in the Southern Ocean. *Marine Chemistry* 35 (1–4), 399–410.
- Dehairs, F., Shopova, D., Ober, S., Veth, C., Goeyens, L., 1997. Particulate barium stocks and oxygen consumption in the Southern Ocean mesopelagic water column during spring and early summer: relationship with export production. *Deep-Sea Research. Part 2. Topical Studies in Oceanography* 44 (1–2), 497–516.
- Dehairs, F., Fagel, N., Antia, A.N., Peinert, R., Elskens, M., Goeyens, L., 2000. Export production in the Bay of Biscay as estimated from barium–barite in settling material: a comparison with new production. *Deep-Sea Research* 47 (4), 583–601.
- Dickey, T., Zedler, S., Yu, X., Doney, S.C., Frye, D., Jannasch, H., Manov, D., Sigurdson, D., McNeil, J.D., Dobeck, L., et al., 2001. Physical and biogeochemical variability from hours to years at the Bermuda Testbed Mooring site: June 1994–March 1998. *Deep-Sea Research. Part 2. Topical Studies in Oceanography* 48 (8–9), 2105–2140.
- Donat, J.R., Lao, K.A., Bruland, K.W., 1994. Speciation of dissolved copper and nickel in South San Francisco Bay—a multi-method approach. *Analytica Chimica Acta* 284 (3), 547–571.
- Dymond, J., Collier, R., 1996. Particulate barium fluxes and their relationships to biological productivity. *Deep-Sea Research. Part 2. Topical Studies in Oceanography* 43 (4–6), 1283–1308.
- Dymond, J., Suess, E., Lyle, M., 1992. Barium in deep-sea sediment: a geochemical proxy for paleoproductivity. *Paleoceanography* 7 (2), 163–181.
- Ebdon, L., Fisher, A., Handley, H., Jones, P., 1993. Determination of trace metals in concentrated brines using inductively coupled plasma mass spectrometry on-line preconcentration and matrix elimination with flow injection. *Journal of Analytical Atomic Spectrometry* 8 (7), 979–981.
- Esser, B.K., Volpe, A.M., 2002a. At-sea high-resolution chemical mapping: extreme barium depletion in North Pacific surface water. *Marine Chemistry*, in press.
- Esser, B.K., Volpe, A.M., 2002b. At-sea high-resolution trace-metal mapping: San Diego Bay and its plume in the coastal ocean. *Environmental Science and Technology*, in press.
- Fagel, N., Andre, L., Dehairs, F., 1999. Advective excess Ba transport as shown from sediment and trap geochemical signatures. *Geochimica et Cosmochimica Acta* 63 (16), 2353–2367.
- Falkner, K.K., Klinkhammer, G.P., Bowers, T.S., Todd, J.F., Lewis, B.L., Landing, W.M., Edmond, J.M., 1993. The behavior of barium in anoxic marine waters. *Geochimica et Cosmochimica Acta* 57, 537–554.
- Falkner, K.K., Macdonald, R.W., Carmack, E.C., Weingartner, T., 1994. The potential of barium as a tracer of Arctic water masses. In: Johannessen, O.M., Muench, R.D., Overland, J.E. (Eds.), *The Polar Oceans and Their Role in Shaping the Global Environment*. American Geophysical Union, pp. 63–76.

- Falkowski, P.G., Barber, R.T., Smetacek, V., 1998. Biogeochemical controls and feedbacks on ocean primary production. *Science* 281 (5374), 200–206.
- Flegal, A.R., Sañudo-Wilhelmy, S.A., 1993. Comparable levels of trace metal contamination in two semi-enclosed embayments: San Diego Bay and south San Francisco Bay. *Environmental Science and Technology* 27 (9), 1934–1936.
- Gieskes, J., Volpe, A., Esser, B., Chen, R., Mahn, C., 2002. Trace metal distributions in San Diego Bay and environments: September 15–16, 1999. *Estuarine, Coastal and Shelf Science*, in preparation.
- Hickey, B.M., 1998. Coastal oceanography of Western North America from the tip of Baja California to Vancouver Island. Robinson, A.R., Brink, K.H. (Eds.), *The Sea, Ideas and Observations on Progress in the Study of the Seas*, vol. 11. Wiley, New York, pp. 345–393.
- Jickells, T.D., 1998. Nutrient biogeochemistry of the coastal zone. *Science* 281 (5374), 217–222.
- Johnson, K.S., Coale, K.H., Jannasch, H.W., 1992. Analytical chemistry in oceanography. *Analytical Chemistry* 64 (22), A1065–A1075.
- Koeve, W., Ducklow, H.W., 2001. JGOFS synthesis and modeling: the North Atlantic Ocean. *Deep-Sea Research. Part 2. Topical Studies in Oceanography* 48 (10), 2141–2154.
- Kupferman, S.L., Livingston, H.D., Bowen, V.T., 1979. A mass balance for ^{137}Cs and ^{90}Sr in the North Atlantic Ocean. *Journal of Marine Research* 37, 157–199.
- Livingston, H.D., 1988. The use of Cs and Sr isotopes as tracers in the Arctic Mediterranean Seas. *Philosophical Transactions of the Royal Society of London* A325, 161–176.
- Livingston, H.D., Bowen, V.T., Casso, S.A., Volchok, H.L., Noshkin, V.E., Wong, K.M., Beasley, T.M., 1985. *Fallout Nuclides in Atlantic and Pacific Water Columns: GEOSECS Data Woods Hole Oceanographic Institution, Woods Hole, MA Technical Report*, 73 pp.
- Lynn, R.J., Simpson, J.J., 1987. The California Current system: the seasonal variability of its physical characteristics. *Journal of Geophysical Research* 92 (C12), 12947–12966.
- Martin, M., 1985. State Mussel Watch: toxics surveillance in California. *Marine Pollution Bulletin* 16 (4), 140–146.
- Mason, R.P., 2001. Trace chemical species in the water column and atmosphere of the Atlantic Ocean. *Deep-Sea Research. Part 2. Topical Studies in Oceanography* 48 (13), 2775–2779.
- McCain, B.B., Chan, S.L., Krahn, M.M., Brown, D.W., Myers, M.S., Landahl, J.T., Pierce, S., Clark, R.C., Varanasi, U., 1992. Chemical contamination and associated fish diseases in San Diego Bay. *Environmental Science and Technology* 26 (4), 725–733.
- McGowan, J.A., Cayan, D.R., Dorman, L.M., 1998. Climate–ocean variability and ecosystem response in the Northeast Pacific. *Science* 281 (5374), 210–217.
- Miller, L.A., Bruland, K.W., 1994. Determination of copper speciation in marine waters by competitive ligand equilibration/liquid–liquid extraction—an evaluation of the technique. *Analytica Chimica Acta* 284 (3), 573–586.
- Moffett, J.W., 1995. Temporal and spatial variability of copper complexation by strong chelators in the Sargasso Sea. *Deep-Sea Research. Part 1. Oceanographic Research Papers* 42 (8), 1273–1295.
- Moffett, J.W., Brand, L.E., Croot, P.L., Barbeau, K.A., 1997. Cu speciation and cyanobacterial distribution in harbors subject to anthropogenic Cu inputs. *Limnology and Oceanography* 42 (5), 789–799.
- National Research Council (Ocean Studies Board), 1998. *Opportunities in Ocean Sciences: Challenges on the Horizon*. National Academy Press, Washington, DC.
- Noshkin, V.E., Wong, K.M., Jokela, T.A., Eagle, R.J., Brunk, J.L., 1978. Radionuclides in the marine environment near the Farallon Islands. Lawrence Livermore National Laboratory, Livermore, CA, p. 17.
- Östlund, G.G., Possnert, G., Swift, J.H., 1987. Ventilation rate of the deep Arctic Ocean from carbon 14 data. *Journal of Geophysical Research* 92 (C4), 3769–3777.
- Paulson, A.J., 1986. Effects of flow rate and pretreatment on the extraction of trace metals from estuarine and coastal seawater by Chelex-100. *Analytical Chemistry* 58, 183–187.
- Rasmussen, L., 1981. Determination of trace metals in seawater by Chelex-100 or solvent extraction techniques and atomic absorption spectrometry. *Analytica Chimica Acta* 125, 117–130.
- Sañudo-Wilhelmy, S.A., Flegal, A.R., 1991. Trace element distributions in coastal waters along the US–Mexican boundary: relative contributions of natural processes vs. anthropogenic inputs. *Marine Chemistry* 33, 371–392.
- Sañudo-Wilhelmy, S.A., Flegal, A.R., 1992. Anthropogenic silver in the southern California Bight: a new tracer of sewage in coastal waters. *Environmental Science and Technology* 26, 2147–2151.
- Sañudo-Wilhelmy, S.A., Flegal, A.R., 1994. Temporal variations in lead concentrations and isotopic composition in the Southern California Bight. *Geochimica et Cosmochimica Acta* 58 (15), 3315–3320.
- Sañudo-Wilhelmy, S.A., Flegal, A.R., 1996. Trace metal concentrations in the surf zone and in coastal waters off Baja California, Mexico. *Environmental Science and Technology* 30 (5), 1575–1580.
- Segovia-Zavala, J.A., Delgadillo-Hinojosa, F., Alvarez-Borrego, S., 1998. Cadmium in the coastal upwelling area adjacent to the California–Mexico border. *Estuarine, Coastal and Shelf Science* 46 (4), 475–481.
- Shaw, T., 1999. The flux of barium to the coastal waters of the southeastern US: importance of submarine groundwater discharge. *Geochimica et Cosmochimica Acta* 62 (18), 3047–3054.
- Stroobants, N., Dehairs, F., Goeyens, L., Vanderheijden, N., Vangrieken, R., 1991. Barite formation in the Southern Ocean water column. *Marine Chemistry* 35 (1–4), 411–421.
- Uppenbrink, J., Hanson, B., Stone, R., 1998. Chemistry and biology of the oceans. *Science* 281 (5374), 189.
- Volpe, A.M., Esser, B.K., Bianchini, G.M., 2001. Real-time ocean chemical measurement: at-sea ICPMS experiments. *Journal of Analytical Atomic Spectrometry* 16 (8), 801–805.
- Volpe, A., Bandong, B., Esser, B.K., Bianchini, G.M., 2002. Radiocesium in North San Francisco Bay and Baja California coastal surface waters. *Journal of Environmental Radioactivity* 60 (3), 365–380.

- Willie, S.N., Iida, Y., McLaren, J.W., 1998. Determination of Cu, Ni, Zn, Mn, Co, Pb, Cd, and V in seawater using flow injection ICP-MS. *Atomic Spectroscopy* 19 (3), 67–72.
- Wong, K.M., Jokela, T.A., Eagle, R.J., Brunk, J.L., Noshkin, V.E., 1992. Radionuclide concentrations, fluxes, and residence times at Santa Monica and San Pedro Basins. *Progress in Oceanography* 20, 353–391.
- Zamzow, H., Coale, K.H., Johnson, K.S., Sakamoto, C.M., 1998. Determination of copper complexation in seawater using flow injection analysis with chemiluminescence detection. *Analytica Chimica Acta* 377 (2–3), 133–144.
- Zirino, A., Lieberman, S.H., Clavell, C., 1978. Measurement of Cu and Zn in San Diego Bay by automated anodic stripping voltammetry. *Environmental Science and Technology* 12 (1), 73–79.
- Zirino, A., Belli, S.L., VanderWeele, D.A., 1998. Copper concentration and Cu-II activity in San Diego Bay. *Electroanalysis* 10 (6), 423–427.